Formation of the 110-K superconducting phase via the amorphous state in the Bi-Sr-Ca-Cu-O system

Donglu Shi, Ming Tang,* K. Vandervoort,† and H. Claus†
Materials Science Division, Argonne National Laboratory, Argonne, Illinois 60439
(Received 19 January 1989)

The thermodynamic and kinetic behavior of both the 85- and 110-K superconducting phases during the crystallization annealing process has been observed and analyzed using x-ray diffraction, magnetic shielding, and resistivity measurements in crystallized Bi-Sr-Ca-Cu-O glasses with nominal compositions $Bi_2Sr_2Ca_2Cu_3O_x$ (2:2:2:3), $Bi_2Sr_2Ca_3Cu_4O_x$ (2:2:3:4), and $Bi_2Sr_2Ca_4Cu_5O_x$ (2:2:4:5). A single superconducting transition near 110 K has been observed in both resistive and magnetization shielding experiments for crystallized samples with 2:2:3:4 and 2:2:4:5 nominal compositions. Eutectic crystallization occurs during annealing of rapidly solidified glass samples. Both the 85-K and Ca_2CuO_3 phases cooperatively nucleate and grow from the amorphous matrix. The 110-K phase subsequently forms at the interfaces between the eutectic products, controlled by calcium and copper diffusion. A phase-change cycling has been observed, during which the 110-K phase increases in volume percent with increasing annealing time at 870 °C in calcium- and copper-rich samples. It then vanishes as annealing is prolonged at the same temperature. This behavior also occurs with different time periods depending on the initial calcium and copper composition of the samples. Microstructural changes associated with such cycling have also been observed. Also discussed are crystallization mechanisms, diffusion phenomena, and related superconducting properties.

INTRODUCTION

Since the discovery[1,2] of high-T_c superconductivity in the Bi-Sr-Ca-Cu-O system, great effort has been made[3–7] to study the structural and electronic properties of the superconducting phases. The orthorhombic unit-cell structures differ in the number of CuO_2 planes (n) in the Bi-Sr-Ca-Cu-O system. For $n=1$, 2, and 3, the c-axis values are 24, 30.7, and 38 Å, respectively, and the corresponding T_c values are <20, 85, and 110 K, respectively.[8–13] These structures have compositions of Bi_2SrCuO_4 ($n=1$, $T_c<20$ K), $Bi_2Sr_2CaCu_2O_x$ ($n=2$, $T_c=85$ K), and $Bi_2Sr_2Ca_2Cu_3O_x$ ($n=3$, $T_c=110$ K); the $Bi_2Sr_2Ca_2Cu_3O_x$ phase has been observed only in multiphase mixtures.[10–14] The multiphase nature greatly complicates the structural determination, and detailed structural features cannot be clearly analyzed. Because of this same problem, T_c values in the zero-resistance state cannot be easily raised to above 100 K in the Bi-Sr-Ca-Cu-O system, and only very limited data are reported.[14] Also, the materials processed by ceramic solid-state sintering techniques possess a very porous matrix which results in poor transport properties. New methods are therefore needed that cannot only isolate the 110-K superconducting phase but also produce highly homogeneous and dense samples.

Syntactic intergrowth has often been observed in Bi-Ca-Sr-Cu-O systems. This phenomenon involves an important phase-transformation process from which the 85-K phase changes to the 110-K phase through complicated diffusion processes. Study of such mechanisms at the microscopic level is particularly important for clarifying the formation of the 110-K phase. The method we reported before[15,16] gives great advantages in studying the intergrowth phenomenon and phase transformations. The samples were melted first and then rapidly solidified to form a high-density and uniform amorphous structure. The amorphous samples were then annealed at high temperatures to crystallize for forming superconducting phases. Since we started with an amorphous state, any phase and microstructural changes could be clearly observed during the highly controllable crystallization process. For example, we found that, for all the starting compositions investigated, the 85-K phase always crystallizes first from the amorphous matrix. Only much later does the 110-K phase precipitate at the interfaces between the 85-K phase and the Ca_2CuO_3 phase through interface diffusion. This technique has enabled us to thoroughly study the crystallization, phase transformation, diffusion, and formation of the 110-K phase in the Bi-Sr-Ca-Cu-O system.

Here we report more detailed results and analysis of crystallized Bi-Sr-Ca-Cu-O glass samples with 2:2:2:3, 2:2:3:4, and 2:2:4:5 nominal compositions. The study of the crystallization process is also reported.

EXPERIMENTAL METHOD

Starting materials of Bi_2O_3, $SrCO_3$, $CaCO_3$, and CuO were weighed in the atomic proportion of 2:2:2:3, 2:2:3:4, and 2:2:4:5. The weighed powders were thoroughly mixed by a wet ball mill in an agate container for 2 h. After milling, the mixed powders were dried and calcined in air at 800 °C for 12 h. The calcined material was placed in a platinum crucible and heated to the melting point for about 10–15 min to ensure complete melting. The molten material was splat quenched onto a copper plate preheated at 200 °C. Extremely dense glass sample plates with

dimensions of $50\times40\times0.5$ mm^3 were then formed for the subsequent crystallization heat treatment. The samples were annealed at 870 °C in air for 1, 3, 5, 7, 10, and 16 days. The heating and cooling rates for all annealing experiments were 27 and 7 °C/min, respectively.

X-ray diffraction data were taken using a Rikagu diffractometer with Cu $K\alpha$ radiation. Electrical resistivity measurements were performed on annealed sample bars of approximately $10\times1.7\times0.5$ mm^3 using a standard four-probe technique involving a computer-controlled, closed-cycle refrigerator system from 10 to 300 K. Leads were soldered with pure indium onto the samples surface. The current density used for the resistivity measurements was 1.2 A/cm^2. Magnetization shielding data were taken using an SHE superconducting quantum interference device (SQUID) magnetometer in an applied field of 2 Oe from 10 to 150 K. The sample was cooled to 10 K in zero field. A magnetic field of 2 Oe was then applied to the sample. The magnetization data were taken as the temperature of the sample was slowly raised to 150 K. More-detailed information about the sample preparation can be found in Refs. 15 and 16.

RESULTS

Some typical electrical resistivity versus temperature data for the 2:2:2:3 samples annealed at 870 °C for 1, 10, and 16 days are shown in Figs. 1(a), 1(b), and 1(c), respectively. As can be seen in this figure, there is a noticeable resistivity drop near 110 K for all three samples, indicating a very small amount of 110-K phase in the material. Resistivity reaches zero at 80 K for all the samples annealed at 870 °C for 1, 3, 5, 7, 10, and 16 days. As also can be seen in the figure, the resistivity at T_c onset $\rho(T_c)$ remains around 2.5 mΩ cm.

The samples with 2:2:3:4 nominal composition exhibit different resistive behavior compared with the 2:2:2:3 samples during the annealing process at 870 °C. The resistivity data for the samples annealed for 1, 10, and 16 days are shown in Figs. 2(a), 2(b), and 2(c), respectively. Here again, the resistivity curve has a large drop at 110 K, and a tail extended to the zero-resistance state at 80 K. The depth of the resistivity drop at 110 K consistently increases with annealing time, and a complete superconducting transition at 110 K is observed for the sample annealed for 10 days [Fig. 2(b)]. However, $\rho(T_c)$ has increased from 1.5 to around 6 mΩ cm. The single resistive transition at 110 K is also observed for the 16-day annealed sample, as shown in Fig. 2(c), and $\rho(T_c)$ has dropped back to 1.5 mΩ cm.

The samples with 2:2:4:5 nominal composition exhibit interesting resistive behavior during the annealing process. For the sample annealed for 1 day at 870 °C, the resistivity curve has a double superconducting transition at 110 and 80 K, with a fairly long tail ending at 60 K, as shown in Fig. 3(a). It then becomes a complete single transition at 110 K with $T_c(\rho=0)$ near 100 K after 3-day annealing [Fig. 3(b)]. Both the 5- and 7-day annealed samples show

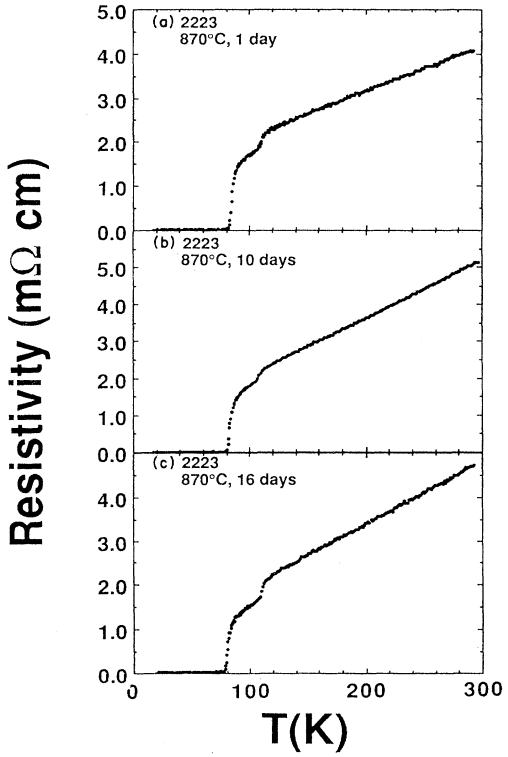

FIG. 1. Resistivity vs temperature for the samples with $Bi_2Sr_2Ca_2Cu_3O_x$ nominal composition annealed at 870 °C for (a) 1 day, (b) 10 days, and (c) 16 days.

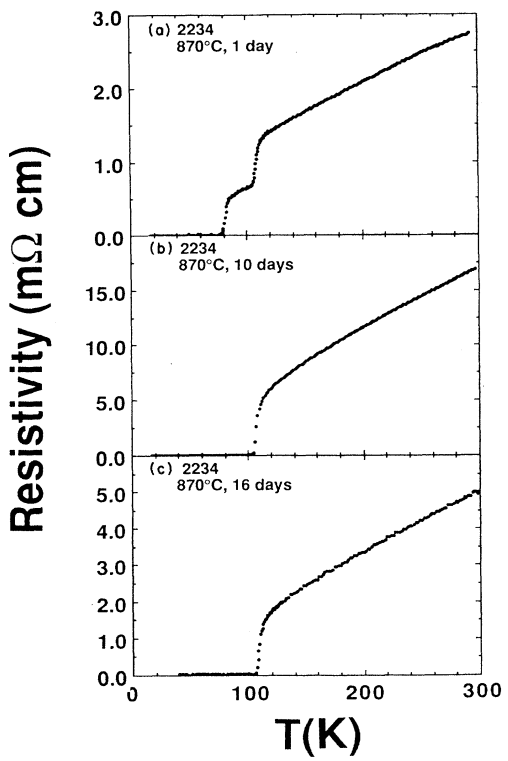

FIG. 2. Resistivity vs temperature for the samples with $Bi_2Sr_2Ca_3Cu_4O_x$ nominal composition annealed at 870 °C for (a) 1 day, (b) 10 days, and (c) 16 days.

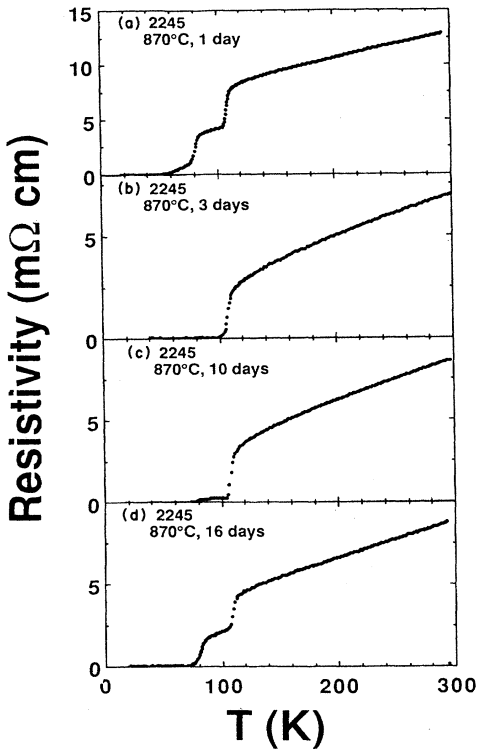

FIG. 3. Resistivity vs temperature for the samples with $Bi_2Sr_2Ca_4Cu_5O_x$ nominal composition annealed at 870 °C for (a) 1 day, (b) 3 days, (c) 10 days, and (d) 16 days.

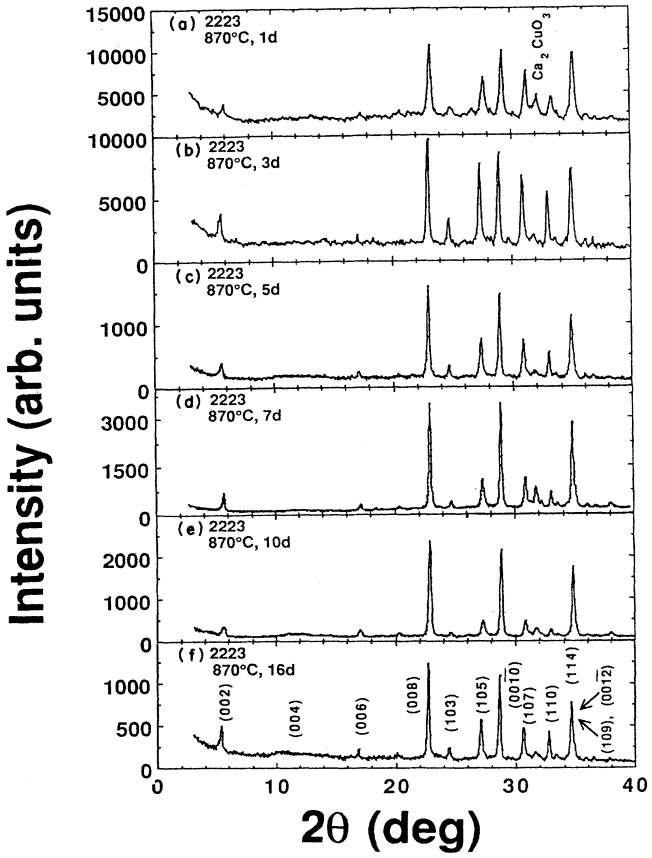

FIG. 4. X-ray diffraction plots for the samples with $Bi_2Sr_2Ca_2Cu_3O_x$ nominal composition annealed at 870 °C for (a) 1 day, (b) 3 days, (c) 5 days, (d) 7 days, (e) 10 days, and (f) 16 days. The index of the 85-K phase is indicated in (f).

similar resistive behavior (double transitions at 110 and 80 K) compared with the 1-day annealed sample (figures are not shown). As annealing time is increased to 10 days, the resistivity curve shows an almost complete transition at 110 K, and a rather small tail which reaches the zero-resistance state at near 80 K [Fig. 3(c)]. As can be seen in Fig. 3(d), the prolonged anneal for 16 days does not enhance the superconducting transition at 110 K. A transition at 80 K has substantially developed, indicating the degrading of the 110-K phase.

X-ray diffraction results are shown in Figs. 4, 5, and 6 for the samples with nominal compositions of 2:2:2:3, 2:2:3:4, and 2:2:4:5, respectively. Indicated in Tables I and II are the 2θ and d-spacing values for the 85- and 110-K phases, respectively. These values are calculated based on unit-cell parameters given in Refs. 9 and 12.

The x-ray diffraction data for the 2:2:2:3 samples annealed at 870 °C for 1, 3, 5, 7, 10, and 16 days are shown in Figs. 4(a), 4(b), 4(c), 4(d), 4(e), and 4(f), respectively. The sample annealed for 1 day shows a 85-K phase plus a small amount of impurity (Ca_2CuO_3). Most of the diffraction peaks intensify and become sharper as the annealing time is prolonged to 3 days; the Ca_2CuO_3 impurity peak is also greatly reduced, showing the mostly single phase (85-K phase) structure at this annealing stage. As annealing time is extended from 3 to 10 days at 870 °C, the relative intensity of (00l) peaks clearly increases, indicating an increased degree of orientation [Figs. 4(c)–4(e)]. At 10 days, this effect reaches a maximum and then decreases with annealing time up to 16 days [Fig. 4(f)].

Figure 5 shows x-ray diffraction plots of the 2:2:3:4 samples annealed at 870 °C for 1, 3, 5, 7, 10, and 16 days. As shown in Fig. 5(a), the sample annealed for 1 day contains mostly the 85-K phase and an impurity phase (Ca_2CuO_3). The 110-K phase peaks (the most noticeable ones are located at $2\theta = 4.65°$ and 23.41°) start to develop after 5 days of annealing [Fig. 5(c)]. The intensity of these peaks [as indicated by the arrows in Fig. 5(d)] then gradually increases with annealing time, showing an increase in volume percent of the 110-K phase [Figs. 5(c)–5(e)]. However, such growth of the 110-K phase ceases after 10 days of annealing. As can be seen in Fig. 5(f), the relative intensity of the (00$\bar{1}$0) diffraction peak has decreased. (This decrease in volume percent of the 110-K phase is confirmed by magnetization shielding data.) It can be seen from Fig. 5 that a similar orientation behavior of the crystalline grains occurs in the annealed 2:2:3:4 samples. It can be clearly seen from Figs. 5(b) through 5(e) that the intensity of non-(00l) peaks is decreasing as annealing time is extended from 3 to 10 days. This decrease indicates possible rapid growth in the a-b plane. Interestingly, such growth is replaced by new

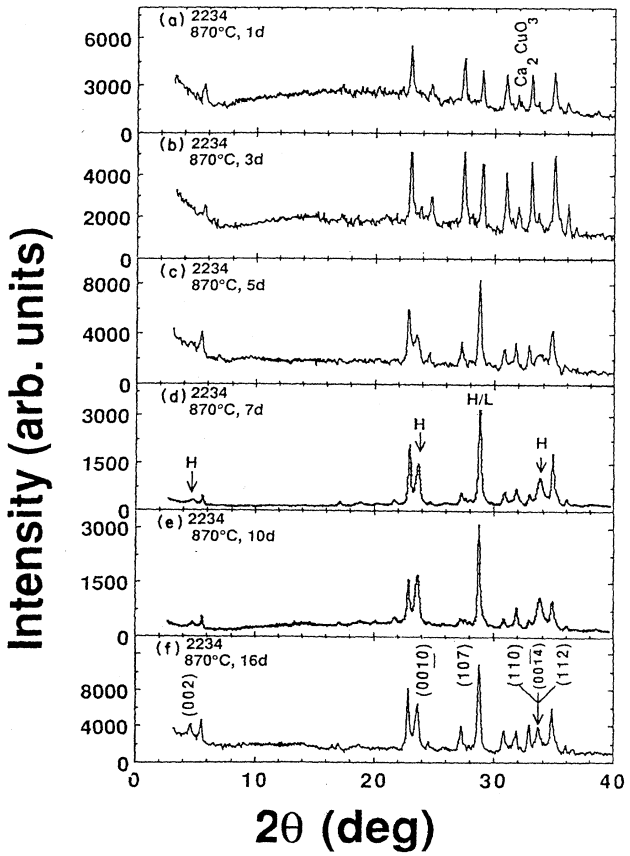

FIG. 5. X-ray diffraction plots for the samples with $Bi_2Sr_2Ca_3Cu_4O_x$ nominal composition annealed at 870 °C for (a) 1 day, (b) 3 days, (c) 5 days, (d) 7 days, (e) 10 days, and (f) 16 days. The index of the 110-K phase [marked as *H* in (d)] is indicated in (f). The highest peak located near $2\theta \approx 29°$ actually contains two peaks belonging to both 110 K (*H*) and 85 K (*L*), therefore marked as *H/L*.

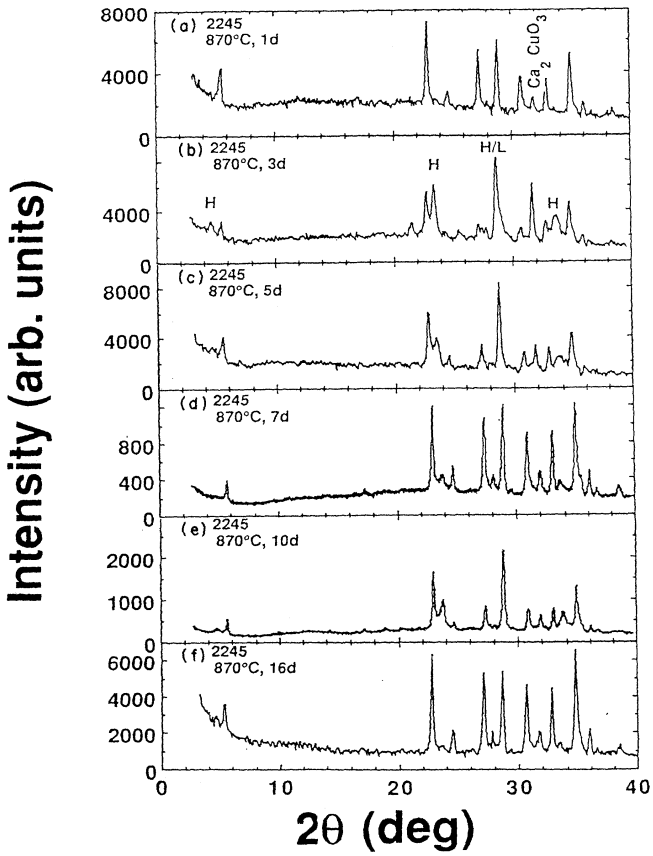

FIG. 6. X-ray diffraction plots for the samples with $Bi_2Sr_2Ca_4Cu_5O_x$ nominal composition annealed at 870 °C for (a) 1 day, (b) 3 days, (c) 5 days, (d) 7 days, (e) 10 days, and (f) 16 days.

TABLE I. 2θ and *d*-spacing values for the 85-K phase. (The values are calculated based on unit-cell parameters given in Refs. 9 and 12.) ($a = b = 3.812$ Å, $c = 30.660$ Å.)

hkl	2θ	*d* (Å)
002	5.76	15.330
004	11.54	7.665
006	17.35	5.110
008	23.21	3.833
101	23.52	3.783
103	24.93	3.572
105	27.55	3.237
0010	29.12	3.066
107	31.10	2.876
110	33.24	2.696
112	33.76	2.655
0012	35.12	2.555
114	35.30	2.543
109	35.33	2.540
116	37.73	2.384

TABLE II. 2θ and *d*-spacing values for the 110-K phase. (The values are calculated based on unit cell parameters given in Refs. 9 and 12.) ($a = b = 3.812$ Å, $c = 38.0$ Å.)

hkl	2θ	*d* (Å)
002	4.65	19.00
004	9.31	9.50
006	13.98	6.33
008	18.68	4.75
0010	23.41	3.80
101	23.45	3.79
103	24.38	3.65
105	26.15	3.41
0012	28.18	3.17
107	28.61	3.12
109	31.62	2.83
0014	33.00	2.71
110	33.24	2.70
112	33.58	2.67
114	34.59	2.59
1011	35.05	2.56
116	36.22	2.48
0016	37.88	2.38
118	38.40	2.34
1013	38.82	2.31

growth after 10 days of annealing, which destroys the platelet grain structure. As shown in Fig. 5(f), the degree of preferred orientation is lessened compared with the sample annealed for 10 days.

X-ray diffraction data of the 2:2:4:5 samples show interesting growth as indicated in Fig. 6. For the sample annealed for 1 day at 870 °C, the data agree with the other two compositions 2:2:2:3 and 2:2:4:5: The 85-K phase crystallizes first from the amorphous matrix. Some impurity of Ca_2CuO_3 has also precipitated. However, the growth of the 110-K phase is much more rapid compared with the 2:2:3:4 samples. As shown in Fig. 6(b), large amounts of the 110-K phase have already formed for the 3-day annealing of 2:2:4:5, while only small amounts of the 110-K phase are present in the comparable case for the 2:2:3:4 sample [Fig. 5(b)]. The amount of the 110-K phase then starts to decrease as annealing is prolonged from 3 to 7 days [shown in Figs. 6(c) and 6(d)]. Interestingly, the 110-K phase grows back as annealing extends from 7 to 10 days [Fig. 6(e)] and almost disappears again after 16-day anneal [Fig. 6(f)]. The entire growth process goes through a phase cycling with a period of approximately 3 days.

We reannealed, for an extra 3 days, a 2:2:4:5 sample at 870 °C that had previously been annealed for 16 days at 870 °C and had mostly the 85-K phase. This sample went through a phase-change cycle, and the x-ray diffraction pattern shows that large amounts of the 110-K phase were formed. This suggests that phase cycling will repeat even for long periods of time at 870 °C.

Another interesting feature is that the preferred orientation effect is again observed in this annealing series. More importantly, the orientation is closely related to the phase changes during the annealing process. We found that the increase of the preferred orientation effect is always accompanied by an increase of the 110-K phase and vice versa [see Figs. 6(a) and 6(b)]. The (00*l*) peaks intensify as the volume percent of the 110-K phase increases. The orientation effect as well as the 110-K phase then decreases as annealing extends from 3 to 7 days. This cycle is repeated as annealing extends from 7 to 16 days. The same phenomenon is seen in the 2:2:3:4 annealing series [Figs. 5(a) through 5(e)], but the cycling period is much longer ($T \sim 10$ days).

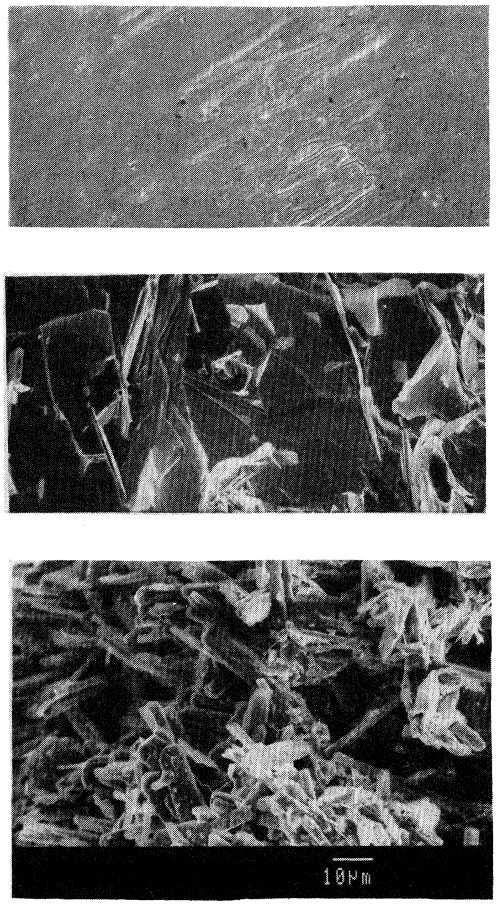

FIG. 7. Scanning electron microscopy photographs (secondary electron) for the samples with $Bi_2Sr_2Ca_3Cu_4O_x$ nominal composition, (a) as-quenched glass, (b) annealed at 870 °C for 10 days, and (c) annealed at 870 °C for 16 days.

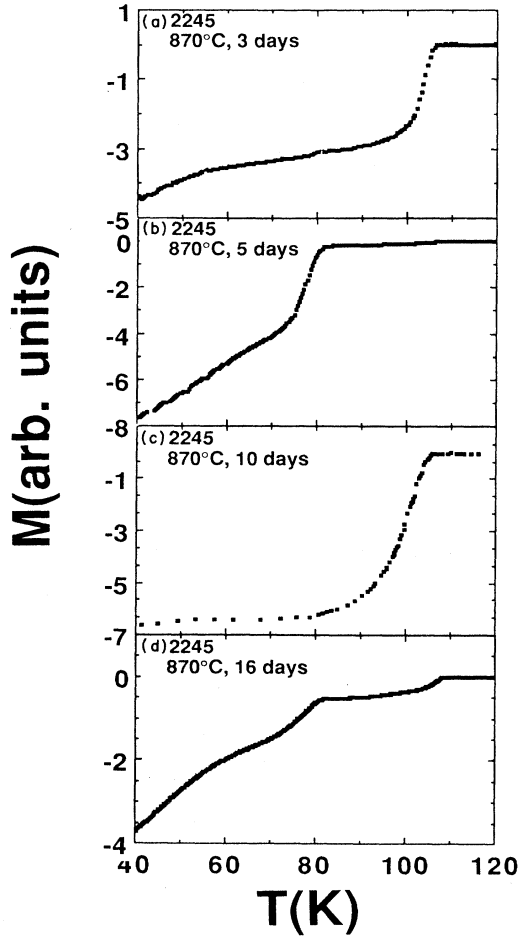

FIG. 8. Zero-field-cooled magnetization vs temperature for the samples with $Bi_2Sr_2Ca_4Cu_5O_x$ nominal composition annealed at 870 °C in air for (a) 3 days, (b) 5 days, (c) 10 days, and (d) 16 days.

Scanning electron microscopy (SEM) photographs of the 2:2:3:4 samples are shown in Fig. 7. The surface of an as-quenched glass sample shown in Fig. 7(a) indicates that rapid solidification results in a very dense and homogeneous material matrix. When the sample is annealed at 870 °C for 10 days, large platelike grains are grown [Fig. 7(b)]. The estimated plate thickness is about 0.5 μm. This is consistent with the x-ray diffraction data that certain texturing is being developed as annealing time extends from 1 to 10 days (Fig. 5). It should be noted that as the texturing increases, so does the volume percent of the 110-K phase. As annealing time at 870 °C is prolonged to 16 days, the platelike grains do not continue to grow; rather, they are replaced by rodlike grains [as shown in Fig. 7(c)]. This fact is also consistent with the x-ray diffraction data that these non-(00l) peaks are developed during anneal from 10 to 16 days at 870 °C [Fig. 5(f)]. Again, the accompanying effect is a decrease in the amount of the 110-K phase. Similar microscopic behavior has also been observed in both the 2:2:2:3 and 2:2:4:5 samples.

Magnetization shielding experimental data are shown in Fig. 8 for the 2:2:4:5 samples annealed at 870 °C for 3, 5, 10, and 16 days. As shown in Fig. 8(a), the 3-day annealed sample exhibits a single superconducting transition onset at 106 K, indicating that the principal phase in the sample is the 110-K phase. This fact is consistent with the x-ray diffraction data shown in Fig. 6(b). As annealing time is extended to 5 days, however, the phase transforms almost entirely to the 80-K phase [Fig. 8(b)]. The phase-change cycle repeats at 10 days, with only a single transition at 110 K [Fig. 8(c)]. The amount of 110-K phase then decreases, and at an annealing time of 16 days the dominant phase in the sample is the 85-K phase [Fig. 8(d)].

The magnetization data of the 2:2:3:4 samples are shown in Fig. 9. From Figs. 9(a) through 9(c), we can see a gradual increase in the volume percent of the 110-K phase as the annealing time extends from 1 to 10 days. After 10 days of annealing, however, the 110-K phase starts to transform into the 85-K phase. As shown in Fig. 9(d), the magnetization signal has a sharp transition at 80 K, indicating the presence of large amounts of the 85-K phase after 16 days of annealing.

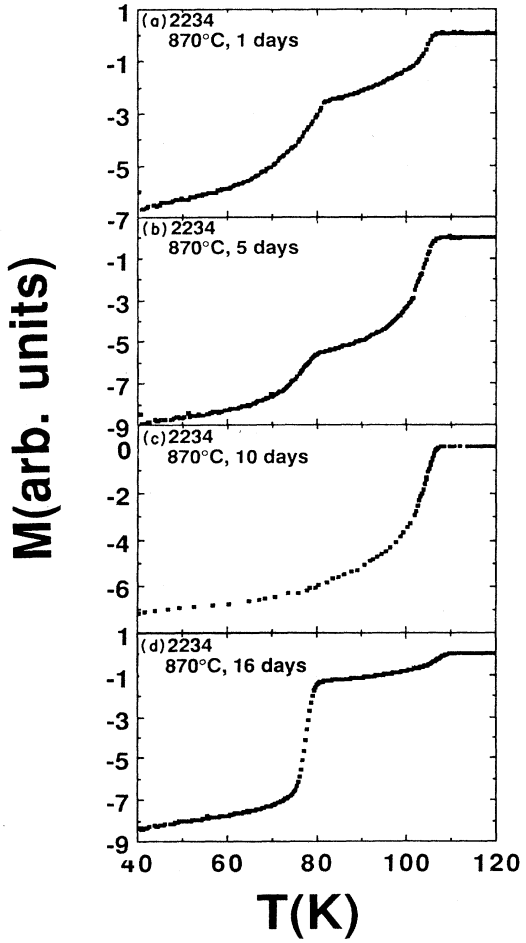

FIG. 9. Zero-field-cooled magnetization vs temperature for the samples with $Bi_2Sr_2Ca_3Cu_4O_x$ nominal composition annealed at 870 °C in air for (a) 1 day, (b) 5 days, (c) 10 days, and (d) 16 days.

DISCUSSION

Crystallization in rapidly solidified Bi-Sr-Ca-Cu-O glass systems appears to occur by nucleation and growth processes. The type of crystallization observed is the so-called eutectic crystallization for the 2:2:2:3 samples. As shown in Fig. 10(a), the rapid splat quenching resulted in a complete amorphous structure. As the amorphous sample was heated at 870 °C for 3 min, it crystallized to two phases: The 85-K phase and Ca_2CuO_3 [Fig. 10(b)]. The transition of the amorphous state into the crystalline phases proceeds by the following sequences: simultaneous crystallization of two crystalline phases $Bi_2Sr_2CaCu_2O_x$

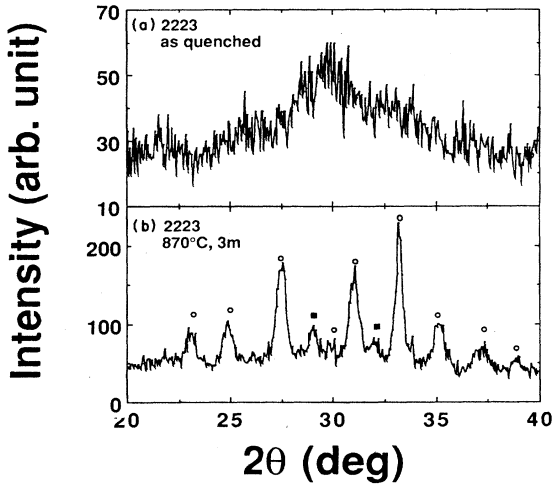

FIG. 10. X-ray diffraction plots for the 2:2:2:3 samples (a) as splat quenched, and (b) the same amorphous sample annealed at 870 °C for 3 min. The O represent x-ray diffraction peaks for the 85-K phase, and ■ for the Ca_2CuO_3 phase.

and Ca_2CuO_3 takes place at the beginning of the crystallization process. As indicated by the x-ray diffraction data, the amount of Ca_2CuO_3 is small for all three compositions (2:2:2:3, 2:2:3:4, and 2:2:4:5) compared with the 85-K phase. For the 2:2:2:3 samples, only very small amounts of the 110-K phase have formed after 24 h of annealing at 870 °C. The volume percent of this phase is estimated to be less than 5% (since it is not shown in the x-ray diffraction patterns, and it has been detected only in the magnetization and resistivity measurements). The 110-K phase is able to grow to a large extent as the calcium and copper contents are increased to the atomic ratio of 2:2:3:4 and 2:2:4:5 in the nominal composition. As calcium and copper contents increase to a higher level such as in the 2:2:3:4 and 2:2:4:5 samples, crystallization may occur through a so-called primary crystallization, during which the calcium- and copper-rich phases precipitate first from the amorphous matrix. An SEM photograph showing calcium- and copper-rich regions in a 2:2:4:5 sample annealed at 870 °C for 3 days is shown in Fig. 11. Eutectic crystallization subsequently takes place when the composition of the matrix has shifted to near eutectic point, which should be close to the nominal composition of the 2:2:2:3 samples.

The explanation for the formation of the 110-K phase is intergrowth process after crystallization. As eutectic crystallization occurs, interfaces between the 85-K phase and Ca_2CuO_3 are created in the typical layered eutectic microstructure. Because of large calcium and copper concentration differences between these two phases, calcium and copper atoms diffuse into the 85-K phase. Therefore, 110-K crystals may nucleate and grow coherently on the 85-K phase matrix by adding one more Cu-O and Ca-O planes to the 85-K phase unit cell. This speculation seems reasonable in that the diffusion process is obviously enhanced by increasing calcium and copper content in the initial composition. The formation of the 110-K phase is much more rapid in the 2:2:4:5 samples. As shown in Figs. 6(a), 6(b), and 8(a) for the 2:2:4:5 samples, the principal phase is the 110-K phase after 3 days of annealing at 870 °C, while in the 2:2:3:4 samples 10 days are needed to reach the maximum amount of the 110-K phase [Fig. 5(e)].

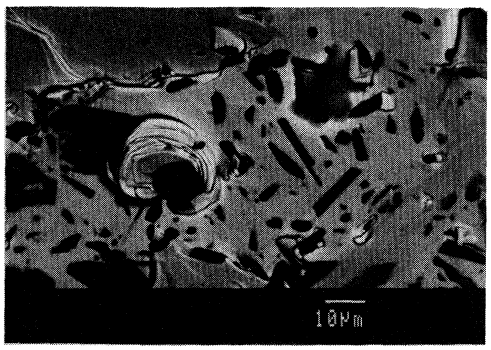

FIG. 11. Scanning electron microscopy photograph (secondary electron) of a 2:2:4:5 sample annealed at 870 °C for 3 days. The dark regions are calcium- and copper-rich phase resulted from primary crystallization.

The phase-change cycle observed from the 2:2:3:4 and 2:2:4:5 samples is of great interest. As stated in the results section, the 110-K phase goes through cycles during the annealing process. In the 2:2:3:4 and 2:2:4:5 samples, the 110-K phase grows with annealing time at 870 °C and then disappears after a certain time period depending on the initial composition. For the 2:2:3:4 samples, the 110-K phase reaches a maximum after 10 days of annealing, and then starts to decrease (Fig. 5). The same behavior is observed in the 2:2:4:5 samples (Fig. 6) although with a different cycling period. The maximums are reached at 3, 10, and 19 days (approximately), showing a much shortened cycling period. One possible explanation is that the 110-K phase at 870 °C is neither thermodynamically nor chemically stable; it tends to segregate into the 85-K and Ca_2CuO_3 phases. As segregation proceeds, the 85-K and Ca_2CuO_3 phases cannot grow any further. The calcium and copper concentration at the interfaces between the 85-K and Ca_2CuO_3 phases reaches equilibrium, at which point a new diffusion mechanism takes place. Specifically, the 110-K phase renucleates and grows at these interface areas, and thereafter the phase-change cycle continues. The phase-change cycle is consistent with our speculation that the cycling period for the 2:2:4:5 samples is much shorter than that of the 2:2:3:4 samples as a result of the increased calcium and copper contents, from which the diffusion process is greatly enhanced.

The microstructures of the annealed samples are found to be closely related to the phase-change cycle. As mentioned in the results section, texturing effects in the x-ray diffraction patterns for all three initial compositions have been observed. By SEM examination, we found that these effects are associated with the growth of platelike grains [Fig. 7(b)]. More important, we found that the growth of the platelike grains is always accompanied by an increase in volume percent in the 110-K phase. As the maximum amount of the 110-K phase is reached, the planelike grains have also grown to the maximum size. As annealing proceeds, the platelike grains are replaced by rodlike grains [Fig. 7(c)], the amount of the 110-K phase accordingly decreases, and the 85-K phase dominates.

The transformation of the platelike grains into the rodlike grains is possibly associated with eutectic crystallization. Eutectic crystallization has been found to occur during the annealing process. One of the fundamental characteristics of eutectic reactions is that both eutecic product phases cooperatively nucleate and grow. In this study, these two phases are the 85-K phase and Ca_2CuO_3. If a Ca_2CuO_3 nucleus forms on a defect in the amorphous matrix, the 85-K phase will nucleate at the interface between the Ca_2CuO_3 and amorphous phases. Lamellae (sheets) of the 85-K and Ca_2CuO_3 can form and advance together into the unstable amorphous matrix. The nucleation processes therefore involve the nucleation of two phases side by side. The 110-K phase may subsequently form at the interfaces between the 85-K phase and Ca_2CuO_3. Because of the eutectic morphology of the initially crystallized 85-K phase and Ca_2CuO_3 lamellae mi-

crostructure, the 110-K phase should also have sheetlike features growing between the 85-K phase and Ca_2CuO_3. Therefore, in a fully grown platelike grain, the 85-K phase can grow from thin sheets into rodlike grains; in fact, the platelike grains may disintegrate as the 2:2:1:2 phase grows. A more detailed crystallization mechanism study of the Bi-Sr-Ca-Cu-O system is underway.

CONCLUSIONS

A single superconducting transition at 110 K has been reproducibly observed in both resistive and magnetization shielding experiments from crystallized Bi-Sr-Ca-Cu-O glasses with 2:2:3:4 and 2:2:4:5 nominal compositions. The crystallization processes have been studied in detail in rapidly solidified, bismuth-based high-T_c superconductors. It is concluded that the 110-K superconducting phase can be obtained through the amorphous state by an appropriate annealing procedure. Both the initial composition of the starting materials and the heat treatment parameters are essential in obtaining the 110-K phase.

Crystallization has been found to occur by nucleation and growth processes. Eutectic and primary crystallization has been observed during the annealing process. The 85-K and Ca_2CuO_3 phases coprecipitate from the amorphous matrix, the 110-K phase subsequently nucleates and grows at the interfaces between the eutectic products. The growth of the 110-K phase is highly controlled by interface diffusion, and the diffusion process is greatly enhanced by increasing the calcium and copper levels of the initial composition. We have observed phase-change cycling and associated microstructural changes. We conclude that the cycling is due to rapid interface diffusion and phase instability and that the grain morphology change is related to the eutectic crystallization.

ACKNOWLEDGMENTS

We are grateful to Shiyou Pei for valuable discussions and some x-ray diffraction data processing. One of the authors (M.T.) is financially supported by the National Science Foundation and the Wisconsin Alumni Research Fund, and would like to thank Dr. Marshall Onellion for useful conversations. This research is supported by the U.S. Department of Energy, Basic Energy Sciences–Materials Sciences, under Contract No. W-31-109-ENG-38.

---

*Present address: Department of Physics, Materials Science Program and Synchrotron Radiation Center, University of Wisconsin, Madison, WI 53706.

†Present address: Department of Physics, University of Illinois at Chicago, Chicago, IL 60680.

[1]C. Michel, M. Herrien, M. M. Borel, A. Grandin, F. Deslandes, J. Provost, and B. Raveau, Z. Phys. B **68**, 421 (1987).

[2]H. Maeda, Y. Tanaka, M. Fukutomi, and T. Asano, Jpn. J. Appl. Phys. Lett. **27**, L209 (1988).

[3]S. S. P. Parkin, V. Y. Lee, A. I. Nazzal, R. Savoy, R. Beyers, and S. J. LaPlaca, Phys. Rev. Lett. **61**, 750 (1988).

[4]R. M. Hazen, C. T. Prewitt, R. J. Angel, N. L. Ross, L. W. Finer, C. G. Hadidiacos, D. R. Veblen, P. J. Heany, P. H. Hor, R. L., Meng, Y. Y. Sun, Y. Q. Wang, Y. Y. Xue, Z. J. Huang, L. Gao, J. Bechtold, and C. W. Chu, Phys. Rev. Lett. **60**, 1174 (1988).

[5]M. A. Subramanian, C. C. Torardi, J. C. Calabrese, J. Gopalakrishnan, K. J. Morrissey, T. R. Askew, R. B. Flippen, U. Chowdhry, and A. W. Sleight, Science **239**, 1015 (1988).

[6]S. A. Sunshine, T. Siegrist, L. F. Schneemeyer, D. W. Murphy, R. J. Cava, B. Batlogg, R. B. van Dover, R. M. Flemming, S. H. Glarum, S. Nakahara, R. Farrow, J. J. Krajewski, S. M. Zahurak, J. V. Waszczak, J. H. Marshall, P. Marsh, L. W. Rupp, Jr., and W. F. Peck, Phys. Rev. B **38**, 893 (1988).

[7]I. K. Schuller and J. D. Jorgensen, Mater. Res. Bull. **XIV**, 24 (1989).

[8]H. W. Zandbergen, Y. K. Huang, M. J. V. Menken, J. N. Li, K. Kadowaki, A. A. Menovsky, G. Van Tendeloo, and S. Amelinckx, Nature (London) **332**, 620 (1988).

[9]H. W. Zandbergen, P. Goren, G. Van Tendeloo, J. Van Landuyt, and S. Amelinckx, Solid State Commun. **66**, 397 (1988).

[10]J. M. Tarascon, Y. LePage, P. Barboux, B. G. Bagley, L. H. Green, W. R. McKinnon, G. W. Hull, M. Girondi, and D. M. Hwang, Phys. Rev. B **37**, 9382 (1988).

[11]R. M. Hazen, C. T. Prewitt, R. G. Angel, N. L. Roy, L. W. Finger, C. G. Hadidiacos, D. R. Veblen, P. J. Heaney, P. H. Hor, R. L. Meng, Y. Y. Sun, Y. Q. Wang, Y. Y. Xua, Z. J. Huang, L. Gao, J. Bechtold, and C. W. Chu, Phys. Rev. Lett. **60**, 1174 (1988).

[12]J. B. Torrance, Y. Tokura, S. J. Laplaca, T. C. Huang, R. J.Savoy, and A. I. Nazzal, Solid State Commun. **66**, 703 (1988).

[13]A. Sumiyama, T. Yoshitomi, H. Endo, J. Tsuchiya, N. Kijima, M. Miznno, and Y. Oguri, Jpn. J. Appl. Phys. **27**, 542 (1988).

[14]B. W. Veal, H. Claus, J. W. Downey, A. P. Paulikas, K. G. Vandervoort, J. S. Pan, and D. J. Lam, Physica C **156**, 635 (1988).

[15]D. Shi, M. Blank, M. Patel, D. G. Hinks, and A. W. Mitchell, Physica C **156**, 822 (1988).

[16]D. G. Hinks, L. Soderholm, D. W. Capone II, B. Dabrowski, A. W. Mitchell, and D. Shi, Appl. Phys. Lett. **53**, 423 (1988).

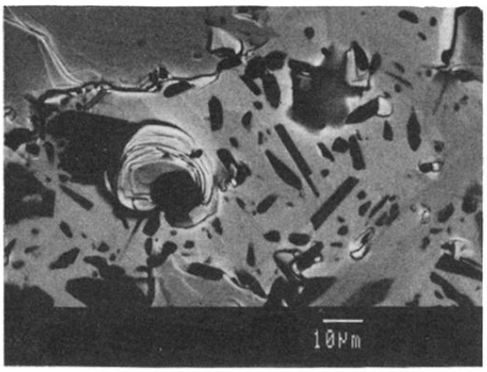

FIG. 11. Scanning electron microscopy photograph (secondary electron) of a 2:2:4:5 sample annealed at 870 °C for 3 days. The dark regions are calcium- and copper-rich phase resulted from primary crystallization.

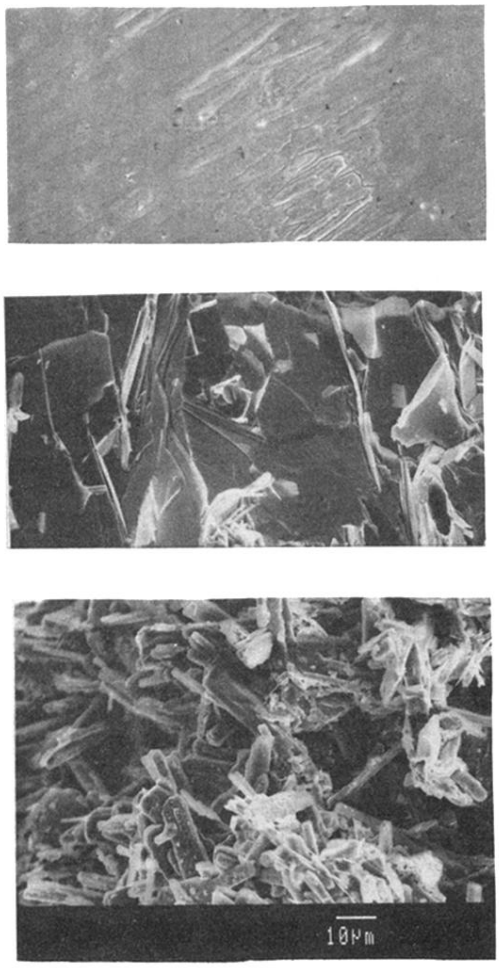

FIG. 7. Scanning electron microscopy photographs (secondary electron) for the samples with $Bi_2Sr_2Ca_3Cu_4O_x$ nominal composition, (a) as-quenched glass, (b) annealed at 870 °C for 10 days, and (c) annealed at 870 °C for 16 days.